PROPERTIES OF THE RESIDUAL STRESS OF THE TEMPORALLY FILTERED NAVIER-STOKES EQUATIONS

C. D. Pruett
Department of Mathematics & Statistics,
James Madison University
Harrisonburg, VA 22807, USA
dpruett@math.jmu.edu

T. B. Gatski
Computational Modeling & Simulation Branch,
NASA Langley Research Center
Hampton, VA 23681, USA
t.b.gatski@larc.nasa.gov

C. E. Grosch
Departments of Ocean, Earth & Atmospheric Sciences and Computer Science,
Old Dominion University
Norfolk, VA 23529, USA
enright@ccpo.odu.edu

W. D. Thacker
Department of Physics, Parks College,
Saint Louis University
St. Louis, MO 63156, USA
thackerw@axa.slu.edu

ABSTRACT

The development of a unifying framework among direct numerical simulations, large-eddy simulations, and statistically averaged formulations of the Navier-Stokes equations, is of current interest. Toward that goal, the properties of the residual (subgrid-scale) stress of the *temporally* filtered Navier-Stokes equations are carefully examined. Causal time-domain filters, parameterized by a temporal filter width $0 < \Delta < \infty$, are considered. For several reasons, the differential forms of such filters are preferred to their corresponding integral forms; among these, storage requirements for differential forms are typically much less than for integral forms and, for some filters, are independent of Δ. The behavior of the residual stress in the limits of both vanishing and infinite filter widths is examined. It is shown analytically that, in the limit $\Delta \to 0$, the residual stress vanishes, in which case the Navier-Stokes equations are recovered from the temporally filtered equations. Alternately, in the limit $\Delta \to \infty$, the residual stress is equivalent to the long-time averaged stress, and the Reynolds-averaged Navier-Stokes equations are recovered from the temporally filtered equations. The predicted behavior at the asymptotic limits of filter width is further validated by numerical simulations of the temporally filtered forced, viscous Burger's equation. Finally, finite filter widths are also considered, and *a priori* analyses of temporal similarity and temporal approximate deconvolution models of the residual stress are conducted.

INTRODUCTION

The Navier-Stokes equations can be solved numerically to predict turbulent flows; however, due to the enormous computational expense required to extract a solution from these equations for flows of engineering interest, it has been necessary in most cases to revert to alternate formulations. For current purposes, three computational approaches are considered: direct numerical simulation (DNS), large--eddy simulation (LES), and Reynolds-averaged Navier--Stokes (RANS) computations. These differ primarily in the level of approximation required to achieve closure.

For LES, the separation of the field variables into resolved and unresolved (spatial) scales is effected by filtering the fields with a low-pass filter. Filtering the momentum equations generates residual (subgrid-scale) stresses that require closure either by modeling or approximation. Recent advances such as dynamic modeling (Germano, 1991) and deconvolution methods (Domaradzki and Saiki 1997, Stolz and Adams 1999) have made LES practical for application to certain flows of engineering interest (Moin and Jimenez, 1993).

Long-time averaging of the Navier-Stokes equations results in the RANS equations for the time-independent mean state. RANS methodology is generally applied to statistically steady flows. To close the system of equations, a model is needed for the Reynolds-stress tensor. Although RANS is computationally appealing, it places a heavy burden on the Reynolds-stress model, which must incorporate the effects of all the unsteady motions upon the mean.

While the formal linkage of the LES and RANS equations

has been well established (Germano 1999, 2001), it is of interest to investigate whether this linkage can be extended practically by developing filtering and averaging procedures that yield mutually consistent solution fields. A possible unifying context for these methodologies is afforded by filter theory. However, the linkage between LES and RANS may be more natural within the context of time-domain filtering rather than the traditional spatial filtering commonly used in LES. Accordingly, the present study focuses on the temporally filtered Navier-Stokes (TFNS) equations and the resultant residual-stress fields.

In the next section causal time-domain filters are discussed, and differential forms are derived for two candidate filters: an exponential filter and a Heaviside filter. The TFNS equations are formulated and analyses of the asymptotic behaviors of the residual stress for limiting values of filter width are presented. Finally, temporal residual-stress models are proposed for the case of finite filter width. Finally, the numerical solution of the forced, viscous Burger's equation is used to further validate the analytical results as well as to evaluate the proposed temporal residual-stress models by *a priori* analyses.

TEMPORALLY FILTERED NAVIER-STOKES EQUATIONS

Time-domain filters are classified as *causal* or *acausal* depending upon whether they are applicable to real-time or *a posteriori* data processing, respectively. The interest here lies in real-time applications for which only causal filtering is appropriate; accordingly, the focus in this study is restricted to causal filters. While aspects of time-domain filters have been discussed previously in this context (Pruett 2000), it is worthwhile to reiterate some fundamental relationships for completeness.

Let $f(t)$ be a continuous function of time t. A causal linear filter is readily constructed by the integral operator

$$\bar{f}(t;\Delta) = \int_{-\infty}^{t} G(\tau - t;\Delta) f(\tau) d\tau, \tag{1}$$

where G is a parameterized filter kernel, and the parameter Δ is the filter width. In general, admissible kernels must satisfy the following property:

$$G(t;\Delta) \equiv \frac{1}{\Delta} g\left(\frac{t}{\Delta}\right), \tag{2}$$

where g is any integrable function such that

$$g(t) \geq 0, \qquad \int_{-\infty}^{0} g(t) dt = 1 \quad \text{and} \quad g(0) = 1. \tag{3}$$

The non-negativity and normalization constraints in Eq. (3) imply that

$$\lim_{t \to -\infty} g(t) = 0, \tag{4}$$

and suffice for G to approach a Dirac delta function as its parameter $\Delta \to 0$; that is,

$$\begin{aligned} \lim_{\Delta \to 0} \bar{f}(t;\Delta) &= \lim_{\Delta \to 0} \int_{-\infty}^{t} G(\tau - t;\Delta) f(\tau) d\tau \\ &= \int_{-\infty}^{t} \delta(\tau - t) f(\tau) d\tau \\ &= f(t). \end{aligned} \tag{5}$$

Two examples of simple, useful filters are obtained by use of an exponential function and a Heaviside function as kernels. For the exponential function, the kernel is

$$g(t) = \exp(t) \to G(t;\Delta) = \frac{\exp(t/\Delta)}{\Delta}, \tag{6}$$

and the resulting integral operator in Eq. (1) is

$$\bar{f}(t;\Delta) = \frac{1}{\Delta} \int_{-\infty}^{t} \exp\left(\frac{\tau - t}{\Delta}\right) f(\tau) d\tau. \tag{7}$$

If $g(t) = h(t+1)$, with h the Heaviside function, then

$$\bar{f}(t;\Delta) = \frac{1}{\Delta} \int_{t-\Delta}^{t} f(\tau) d\tau. \tag{8}$$

A drawback of the integral formulations just presented is the need to retain the long-time history of the solution field. However, by considering instead differential forms of the filter operators, storage requirements are reduced significantly, subject to the intrinsic storage needs of the numerical time-advancement scheme itself (for example, low-storage Runge-Kutta). By differentiating Eqs. (7) and (8), the differential forms of the exponential and Heaviside filters are given by

$$\frac{\partial}{\partial t} \bar{f}(t;\Delta) = \frac{f(t) - \bar{f}(t;\Delta)}{\Delta}, \text{and} \tag{9}$$

$$\frac{\partial}{\partial t} \bar{f}(t;\Delta) = \frac{f(t) - f(t-\Delta)}{\Delta}, \tag{10}$$

respectively.

When causal filtering is applied to a temporally discretized problem with a time increment of Δt, the action of the filter is naturally parameterized by the filter-width ratio r defined as

$$r = \frac{\Delta}{\Delta t}. \tag{11}$$

In order to illustrate the discrete differential filtering process, a 2π-periodic time series is processed by the exponential differential filter given in Eq. (9). The time series is generated from a -3/2 power-law decay in Fourier frequency space, and the phases are assigned randomly. The continuous signal is then sampled at a rate of 512 per period and replicated for three periods. The filtered time series, $\bar{f}$, is then generated by solving Eq. (9) from the initial condition $\bar{f}(0;\Delta) = f(0)$. There are many appropriate numerical integration schemes. Because the right-hand side of the differential form of a linear filter is itself linear, fully implicit Adams-Moulton methods are particularly attractive because of their accuracy and efficiency. Here, standard fourth-order Adams-Moulton methodology is used. The method is started with initial steps of orders one, two, and three, respectively.

The filter-width ratio, r, is the only parameter of the differential filter. In general, the larger the value of r, the more dissipative the filter. (In this context, a "dissipative" low-pass filter is one with significant and broad-band attenuation of high-frequency Fourier harmonics.) The method remains viable for all values of filter-width ratio ($0 < r$). For $r \approx 0$, the evolution equation becomes stiff, and small time steps are necessary. Figure 1 compares the filtered time series with the unfiltered signal for selected values of the filter-width ratio r. As r increases, the output time series becomes smoother and its amplitude diminishes due to the removal of energy at the higher frequencies. As is typical for causal filters, high levels of numerical dissipation generate significant phase lag in the output relative to the input. Figure 2 compares the input signal with the original out-

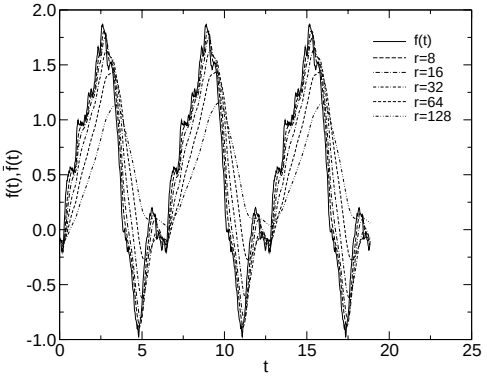

Figure 1: Differentially filtered time series $f(t)$.

put signal and with an output that is phase compensated by r time steps. The phase-compensated signal is an excellent representation of the input, minus its high-frequency components.

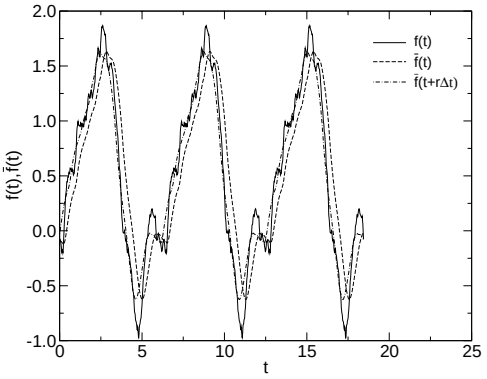

Figure 2: Original, exponentially filtered, and phase-compensated time series $f(t)$ for $r = 32$.

Temporal, causal filtering of the Navier-Stokes equations using Eq. (1) leads to the following form of the TFNS equations:

$$\frac{\partial \overline{u}_j}{\partial x_j} = 0 \tag{12}$$

$$\frac{\partial \overline{u}_i}{\partial t} + \frac{\partial (\overline{u}_i \overline{u}_j)}{\partial x_j} = -\frac{\partial \overline{p}}{\partial x_i} + \nu \frac{\partial^2 \overline{u}_i}{\partial x_j \partial x_j} - \frac{\partial [\tau_{\rm R}]_{ij}}{\partial x_j}, \tag{13}$$

where u_i is the velocity, p is the pressure, and ν is the kinematic viscosity. An overbar denotes a temporal grid-filtered quantity, and $[\tau_{\rm R}]_{ij}$ represents the temporal residual-stress tensor defined as

$$[\tau_{\rm R}]_{ij} \equiv \overline{u_i u_j} - \overline{u}_i \overline{u}_j. \tag{14}$$

Provided that filtering and differentiation operations commute, the TFNS equations are *formally* identical to the spatially filtered Navier-Stokes equations. As pointed out previously by Pruett (2000), commutativity is natural for temporal filters but remains problematic for spatial ones (Blaisdell 1997, Vasilyev et al. 1998). It is now recognized (Pruett 2001, Pruett et al. 2001, De Stefano and Vasilyev 2001) that this formal equivalence does *not* imply quantitative equivalence of the residual-stress fields. In general, for spatial *or* temporal grid filters, the residual stress depends strongly upon the filter, particularly upon its filter width and order property, which influence both the magnitude and the distribution of the residual stress. The implication of this growing awareness is that the residual-stress model cannot be independent of the choice of the filter. To make explicit its formal dependence upon the specific temporal filter, the residual stress is denoted by $[\tau_{\rm R}]_{ij}(\Delta)$ where appropriate.

Limiting Behaviors

Of interest is the effect of filter width Δ on the residual stress $[\tau_{\rm R}]_{ij}$. It is easily shown that the $[\tau_{\rm R}]_{ij}$ vanishes in the limit $\Delta \to 0$. In this limit, the kernel function reduces to a Dirac delta function (see Eq. (5)) so that

$$\lim_{\Delta \to 0} [\tau_{\rm R}]_{ij}(t,x;\Delta) = \lim_{\Delta \to 0} (\overline{u_i u_j} - \overline{u}_i \overline{u}_j) = \lim_{\Delta \to 0} (u_i u_j - u_i u_j) = 0. \tag{15}$$

The vanishing of the temporal residual stress, coupled with the replacement of the other filtered quantities by their unfiltered counterparts, leads to the recovery of the Navier-Stokes equations from the TFNS equations in the limit $\Delta \to 0$.

The other limit of interest is $\Delta \to \infty$. However, before examining the behavior of the residual stress in this limit, it is useful to examine some characteristics of the filtered velocity field itself. It follows from the differential forms of either the exponential or Heaviside differential filters given in Eqs. (9) or (10) that

$$\lim_{\Delta \to \infty} \frac{\partial \bar{u}_i}{\partial t}(t,x;\Delta) = 0, \tag{16}$$

where both u_i and $\bar{u}_i$ are assumed bounded. The condition above establishes that $\bar{u}_i(t,x;\infty)$ is actually independent of time t. (In fact, for Eq. (16) to hold, it suffices that u_i is bounded and that $|g'(t)|$ is integrable on $(-\infty, 0]$. Thus, Eq. (16) applies to a wide class of filters.) For the causal temporal filter defined in Eq. (1) with the Heaviside kernel (for convenience), $\bar{u}_i(t,x;\infty)$ can be written as

$$\lim_{\Delta \to \infty} \bar{u}_i(t,x;\Delta) = \bar{u}_i(0,x;\infty) = \lim_{\Delta \to \infty} \frac{1}{\Delta} \int_{-\Delta}^{0} u_i(\tau,x) d\tau \tag{17}$$

Equation (17) holds for any filter for which $H(0) = 1$, which is typical of low-pass filters. The right-hand-side of Eq. (17) simply defines the long-time average of the variable $u_i(t,x)$, which, for a stationary process, is equivalent to the ensemble average according to the ergodic hypothesis. That is, for a stationary flow

$$\bar{u}_i(0,x;\infty) = E\{u_i(t,x)\}, \tag{18}$$

where $E\{\ \}$ denotes the expected value (or ensemble average). However, Eq. (16) has shown that $\bar{u}_i(t,x;\infty)$ is constant with respect to time so that

$$\bar{u}_i(t,x;\infty) = \bar{u}_i(0,x;\infty) = E\{u_i(t,x)\} = U_i(x), \tag{19}$$

and

$$\lim_{\Delta \to \infty} \frac{\partial}{\partial t} \overline{u}_i(t,x;\infty) = \frac{\partial}{\partial t} E\{u_i(t,x)\} = 0. \tag{20}$$

In the current time-filtered approach, Eq. (19) provides the link between the resolved motions of the variable $u_i(t,x)$ and the ensemble mean $U_i(x)$. Because the variable $u_i(t,x)$ can be partitioned either into a sum of resolved $\bar{u}_i(t,x;\infty)$ and temporally unresolved motions $\tilde{u}_i(t,x)$, or into a sum of time mean $U_i(x)$ and fluctuating $u_i'(t,x)$ quantities, it follows from Eq. (19) that

$$\tilde{u}_i(t,x;\infty) = u_i'(t,x). \tag{21}$$

In addition to the equality between the resolved and mean fields in the limit, Eq. (21) shows the linkage between the

temporally unresolved and fluctuating motions. With these results, it is now possible to examine the limiting behavior of the residual stress.

By the linearity of the filter operator, the residual stress defined in Eq. (14) can be written as

$$\lim_{\Delta\to\infty}[\tau_R]_{ij}(\Delta) = \lim_{\Delta\to\infty}\left[(\overline{\overline{u}_i\overline{u}_j}+\overline{\overline{u}_i\tilde{u}_j} + \overline{\tilde{u}_i\overline{u}_j}+\overline{\tilde{u}_i\tilde{u}_j}) - \overline{u}_i\overline{u}_j\right], \quad (22)$$

where the instantaneous velocity field has been partitioned into resolved and unresolved parts. Because Eqs. (18) and (19) establish an equality between the resolved and ensemble mean fields, and the residual and fluctuating fields, respectively, Eq. (22) can be simplified to

$$\begin{aligned}\lim_{\Delta\to\infty}[\tau_R]_{ij}(\Delta) &= E\{u_j'E\{u_i\}+u_i'E\{u_j\}+u_i'u_j'\}\\ &= E\{u_i'u_j'\}=\tau_{ij}. \end{aligned}\quad (23)$$

That is, for a stationary flow the residual stress ($[\tau_R]_{ij}$) asymptotically approaches the Reynolds stress (τ_{ij}) as $\Delta\to\infty$.

Finite Filter Width

For finite filter width, the residual stress represents the dynamics of a broad spectral range of motions. The TFNS equations provide a governing set of equations suitable for time-filtered LES (Pruett, 2000) (or TLES), for which (accurate) modeling of $[\tau_R]_{ij}$ is required for closure.

The temporal variants of two well-known residual-stress models for $[\tau_R]_{ij}$ are considered: Bardina's scale-similarity model (Bardina et al., 1980) (SSM); and the approximate deconvolution model (ADM) of Stolz and Adams (1999). The time-filtered counterparts of these models are referred to as the temporal scale-similarity model (TSSM) and the temporal approximate deconvolution model (TADM), respectively.

Consider first a TSSM that is formally equivalent to the Bardina model (Bardina et al., 1980),

$$[\tau_R]_{ij} \approx \overline{\overline{u}_i\overline{u}_j} - \bar{\bar{u}}_i\bar{\bar{u}}_j, \qquad \text{(TSSM)}. \quad (24)$$

As in the Bardina model, the same (temporal) filter width is used for the primary and secondary (test) filters. Next, the TADM considered is formally equivalent to the second of the ADM models presented by Stolz and Adams (1999),

$$[\tau_R]_{ij} \approx \overline{v_iv_j} - \bar{v}_i\bar{v}_j, \qquad \text{(TADM)}, \quad (25)$$

where v_i is an approximate deconvolution of $\bar{u}_i$; that is, v_i approximates u_i based upon approximately defiltering (deconvolving) $\bar{u}_i$. Following Stolz and Adams, the zeroth- and first-order deconvolutions of $\bar{u}_i$ yield $v_i=\bar{u}_i$ and $v_i = 2\bar{u}_i - \bar{\bar{u}}_i$, respectively. Higher-order (and more accurate) deconvolutions are possible. Note that the TADM (ADM) generalizes the TSSM (SSM), because the zeroth-order deconvolution is the TSSM. (Appropriately, Stolz and Adams (1999) refer to the second of their ADM models as the generalized SSM model.)

In the next section, an *a priori* analysis of the predictive capability of these two residual-stress models will be performed.

FORCED VISCOUS BURGER'S EQUATION

While it is desirable and ultimately necessary to validate the analytical results previously established in simulations of the full TFNS equations, the wide range of parameter values considered here renders such analyses cost prohibitive. However, it is possible to illustrate the dependence of the residual stress upon the temporal filter width, in general, and the asymptotic behaviors discussed previously, in particular, by simulations of a spatially one-dimensional model problem. To this end, consider the forced, viscous Burger's equation (VBE), written in the form

$$\frac{\partial u}{\partial t}+\frac{1}{2}\frac{\partial(u^2)}{\partial x} = \nu\frac{\partial^2u}{\partial x^2}+f(t,x) \quad ; \quad (0<x<2\pi). \quad (26)$$

with $u(t,x)$ a velocity, $f(t,x)$ an imposed forcing function, and ν a viscosity. The initial condition is $u(0,x)=1$. Without forcing, the initial condition results in a velocity field that is constant for all time and space. Moreover, any perturbations of that field decay toward zero, so that constant "stirring" is required to maintain high-intensity fluctuations (Eswaran and Pope, 1988). This equation can be solved accurately by a Galerkin Fourier spectral method in space coupled with classical 4th-order Runge-Kutta time advancement. A Fourier *ansatz* is assumed for u and substituted into the governing equation. This results in a system of coupled ordinary differential equations for the complex Fourier coefficients U_k, $k=-n/2,...,-1,0,+1...,+n/2$. (Due to conjugate symmetry, only $n/2+1$ positive modes are solved for explicitly.) The equations are coupled through their nonlinear terms, which are evaluated exactly in Fourier space by Cauchy products. Hence, explicit de-aliasing is unnecessary.

For this forced case, $n=256$, and each Fourier mode in the band $1\le k\le k_f$ is independently subjected to periodic forcing $F_k(t)$ such that $F_k(t)=A\phi_k\exp(\iota\omega_k t)$ with real frequency $\omega_k=k\omega$. The band limit $k_f=32$, the fundamental frequency $\omega=1$, and the amplitude $A=0.4$ (the same for all modes) are input parameters, and the time increment is 0.005 throughout. The complex phases $\phi_k=\exp(\iota\alpha_k)$ are assigned initially by random numbers α_k uniformly distributed on $[0,2\pi]$. Thereafter, they remain fixed. As will be shown, after a long-time evolution, a statistically steady flow results. Because, at small ν, the viscous Burger's equation admits solutions with steep shock fronts, only a moderately large value of ν is practical. For the value $\nu=1/300$ and forcing distribution, the flow is highly resolved in both time and space, with Fourier amplitudes at the highest wavenumbers on the order of 10^{-10}.

Causally filtering the forced VBE results in the following equation, which can be considered as a one-dimensional analog of the TFNS equation given in Eq. (13):

$$\frac{\partial\bar{u}}{\partial t}+\frac{1}{2}\frac{\partial(\bar{u}\bar{u})}{\partial x} = \nu\frac{\partial^2\bar{u}}{\partial x^2}+\bar{f}(t,x)-\frac{1}{2}\frac{\partial[\tau_R]}{\partial x} \quad ; \quad (0<x<2\pi). \quad (27)$$

Filtering results in the appearance of a residual stress given by

$$[\tau_R]=\overline{uu}-\bar{u}\bar{u}. \quad (28)$$

In Fig. 3, the instantaneous unfiltered velocity field, obtained from the solution of Eq. (26) at $t=10$ ($\Delta t=0.005$), is compared with the filtered field, which satisfies Eq. (27), for selected values of the filter-width ratio r. Clearly, filtering in time to remove high frequencies effects the removal of energy at high wavenumbers as well.

As implied previously, the behaviors of the residual stress for limiting values of the temporal filter width Δ are key results of the temporally filtered methodology being studied. To illustrate these predicted behaviors in the limits $\Delta\to0$ and $\Delta\to\infty$, the model problem is particularly useful.

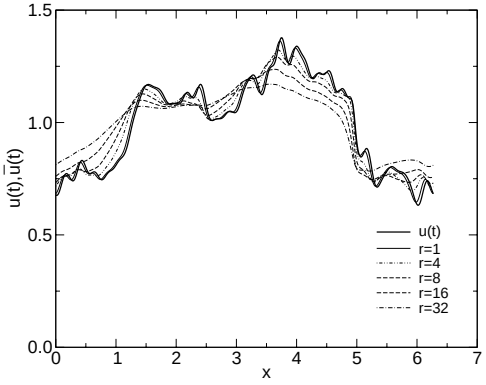

Figure 3: Instantaneous and causally filtered velocity fields at $t = 10$ for filter-width ratios $r = 1$, $r = 4$, $r = 8$, $r = 16$, and $r = 32$.

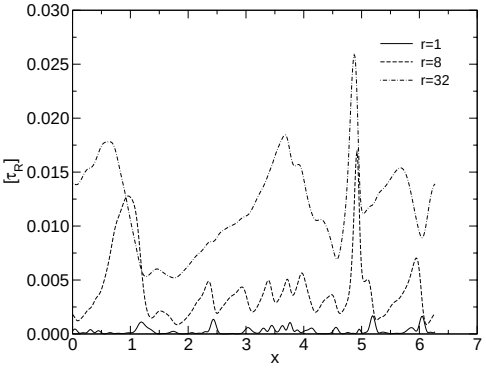

Figure 4: Instantaneous residual stress $[\tau_{\mathrm{R}}]$ at $t = 10$ for filter-width ratios $r = 1$, $r = 8$, and $r = 32$.

Limiting Behavior of Residual Stress

The behavior in the limit $\Delta \to 0$ can be verified numerically by using successively smaller temporal grid-filter widths to process the numerical solution $u(t,x)$ of the VBE. The exact residual stress (28) is evaluated to the accuracy of the numerical scheme by solving, in addition to Eq. (26), the filter evolution equations (cf. Eq. (9))

$$\frac{\partial \overline{u}}{\partial t} = \frac{u - \overline{u}}{\Delta}, \quad \text{and} \quad \frac{\partial \overline{uu}}{\partial t} = \frac{uu - \overline{uu}}{\Delta} \tag{29}$$

from initial conditions $\bar{u}(0,x) = u(0,x)$ and $\overline{uu}(0,x) = u^2(0,x)$. Here, these equations (29) are advanced in time using the standard fourth-order Adams-Moulton method. (The fourth-order Runge-Kutta methodology used to advance the VBE would also be suitable for all the filter equations; however, following the Runge-Kutta update of the solution by the 4th-order Adams-Moulton updates of the filtered quantities has the algorithmic advantage of compartmentalizing the code.) While these Eqs. (29) apply to the exponential filter, an analogous set could be derived for the Heaviside filter.

Figure 4 compares the exact, instantaneous residual stress $[\tau_{\mathrm{R}}]$ at $t = 10$ determined from Eqs. (26) and (29) for selected values of the filter-width ratio r $(= \Delta/\Delta t)$. As expected, the amplitude envelope of the residual stress tends toward zero as r decreases.

The behavior of the velocity and residual stress fields in the limit of $\Delta \to \infty$ can also be analyzed. As was shown in previously, the limiting form of the residual stress $[\tau_{\mathrm{R}}]$ approaches the long-time average stress field τ. While this can be shown by considering successively larger values of the

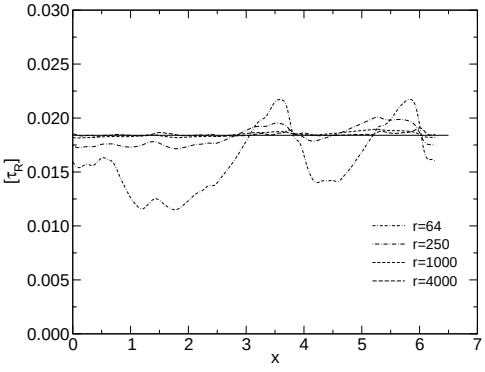

Figure 5: Instantaneous residual stress $[\tau_{\mathrm{R}}]$ at $t = 240$ for selected values of filter-width ratio r: —— long time stress τ.

filter-width ratio r, it is first necessary to establish that the solution of the forced, viscous Burger's equation evolves to a statistically steady (stationary) state. Thus, it is necessary to verify the stationarity of the numerical solution, because the equality of the residual stress and Reynolds stress in the long-time limit is based on this assumption. (See Eqs. (19) and (20).)

The long-time average and the spatial average of the instantaneous velocity field $u(t,x)$ are both equal to unity. The fluctuating field $u'(t,x)$ is extracted at each time step simply by subtracting this mean value from $u(t,x)$. It is verified that the (long-time) solution of the forced viscous Burger's equation is indeed stationary. With the stationarity of the solution of the forced VBE established, it is possible to evaluate the effect of large filter width on the residual stress. In Fig. 5 the long-time averaged stress τ is compared with the instantaneous residual stress $[\tau_{\mathrm{R}}](\Delta)$ at $t = 240$ for different values of the filter-width ratio r. The stress τ is computed by averaging over an interval of duration $\Delta = 20$ during the period in which the flow is essentially stationary ($t = 240$ to 260). As expected, the residual stress $[\tau_{\mathrm{R}}]$, computed in real time using the exponential filter, appears to converge toward the value of τ as Δ becomes large.

Residual Stress for Finite Filter Width

With the limiting behavior of the filter-width Δ on $[\tau_{\mathrm{R}}]$ established for the forced VBE, it remains only to evaluate the behavior of $[\tau_{\mathrm{R}}]$ for finite filter width. As described previously, the exact residual stress is extracted from the solutions of Eqs. (26) and (29). The modeled residual stress can be obtained from these equations by further appending the evolution equations

$$\frac{\partial \overline{\overline{u}}}{\partial t} = \frac{\overline{u} - \overline{\overline{u}}}{\Delta}, \qquad \frac{\partial \overline{\overline{u}\overline{u}}}{\partial t} = \frac{\bar{u}\bar{u} - \overline{\overline{u}\overline{u}}}{\Delta}, \tag{30}$$

and

$$\frac{\partial \bar{v}}{\partial t} = \frac{v - \bar{v}}{\Delta}, \qquad \frac{\partial \overline{vv}}{\partial t} = \frac{vv - \overline{vv}}{\Delta}. \tag{31}$$

Equation (30) is used in conjunction with the TSSM, subject to the initial conditions $\bar{\bar{u}}(0,x) = u(0,x)$ and $\overline{\bar{u}\bar{u}}(0,x) = u^2(0,x)$. For the TADM, both sets, Eqs. (30) and Eq. (31) are involved, subject to the additional initial conditions $\bar{v}(0,x) = u(0,x)$ and $\overline{vv}(0,x) = u^2(0,x)$. As before, these differential filter equations are advanced by the Adams-Moulton method.

In Fig. 6, the exact ($[\tau_{\mathrm{R}}]$) and modeled ($[\tau_{\mathrm{R}}]$(TSSM) and $[\tau_{\mathrm{R}}]$(TADM)) residual stresses are compared at $t = 20$. At this instant, the flow statistics are still evolving in time,

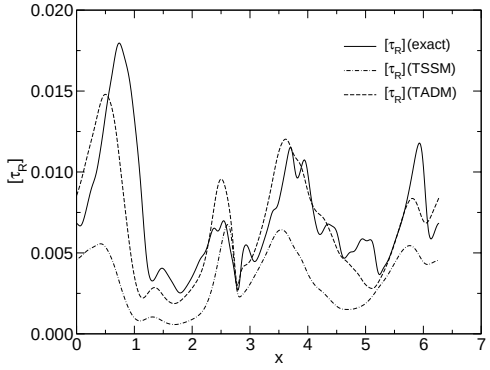

Figure 6: Instantaneous exact and modeled (TSSM, TADM) residual stresses ($[\tau_R]$) at $t = 20$.

for in the finite-Δ case, there is no reason to presuppose stationarity. A fairly dissipative filter of ratio $r = 16$ is used for the *a priori* analysis. Note that for both the exact and modeled residual stresses, $[\tau_R] > 0$ at all times. This realizability property (Vreman et al., 1994) is a consequence of the positivity of the filter kernel established in Eq. (3).

Both the TSSM and TADM correlate relatively well with $[\tau_R]$, with correlation coefficients on the order of 0.8 and 0.9, respectively. Correlations, however, reflect distribution but not amplitude. In general, the TADM has a higher correlation, and its amplitude tends to be more nearly correct. That the TADM performs well with only first-order deconvolution is surprising (as Stolz and Adams (1999) employ 5th order).

CONCLUSIONS

The behavior of the residual stress of the temporally filtered Navier-Stokes (TFNS) equations was studied for a class of differential, causal time-domain filters parameterized by the temporal filter width Δ. The effect of filter width on the residual stress was examined for the asymptotic limits $\Delta \to 0$ and $\Delta \to \infty$ and for the case of finite filter width. It was shown analytically that, in the limit $\Delta \to 0$, the residual stress vanishes so that the Navier-Stokes equations are recovered from the temporally filtered equations. Alternately, in the limit $\Delta \to \infty$, for a statistically steady flow, the residual stress asymptotically approaches the Reynolds stress, and the Reynolds-averaged Navier-Stokes equations are recovered from the temporally filtered equations. These asymptotic results were verified numerically through simulations of the temporally filtered forced, viscous Burger's equation. For the case of finite filter widths, two residual-stress models were considered that are temporal analogs of spatial SGS-stress models. These were a temporal scale similarity model (TSSM) and a temporal approximate deconvolution model (TADM). *A priori* analyses of these models were performed using highly accurate numerical solutions of the filtered forced, viscous Burger's equation. The models were found to approximately replicate the exact residual stress.

It has been shown analytically that the residual stress of the TFNS equations is strongly dependent upon the temporal filter width. This fact, coupled with computational results from simulating the forced, viscous Burger's equation over a wide range of temporal filter widths, suggests that full simulations of the TFNS equations should behave like DNS for small temporal filter widths and like RANS for very large ones. For finite filter widths the formulation describes a temporally filtered LES or TLES. These results have provided a bridging mechanism between solutions obtained directly from the Navier-Stokes equations and those obtained from the Reynolds-averaged Navier-Stokes equations.

ACKNOWLEDGMENTS

CDP and WDT acknowledge the support of NASA Langley Research Center (LaRC) through Grants NAG-1-02033 and NAG-1-02027, respectively. CEG acknowledges the support of NASA LaRC through Grant NAG-1-02005 and the National Science Foundation through Grant NSF OCE-0136403.

REFERENCES

Bardina, J., Ferziger, J. H., and Reynolds, W. C., 1980, "Improved Subgrid-Scale Models for Large Eddy Simulation," *AIAA Paper No. 80-1357.*

Blaisdell, G. A., 1997, "Computation of Discrete Filters and Differential Operators for Large-Eddy Simulation," *Advances in DNS/LES*, C. Liu and Z. Liu (eds.), Greyden Press, Columbus, OH, pp. 333-340.

Stefano, G. D. and Vasilyev, O. V., 2001, "A Study of the Effect of Smooth Filtering in LES," *DNS/LES Progress and Challenges*, C. Liu, L. Sakell, and T. Beutner (eds.), Greyden Press, Columbus, OH, pp. 247-254.

Domaradzki, J. A. and Saiki, E. M., 1997, "A Subgrid-Scale Model Based on the Estimation of Unresolved Scales of Turbulence," *Phys. Fluids A*, Vol. 9, pp. 2148-2164.

Eswaran, V. and Pope, S. B., 1988, "An Examination of Forcing in Direct Numerical Simulations of Turbulence," *Comput. Fluids*, Vol. 16, pp. 257-278.

Germano, M., 1999, "From RANS to DNS: Toward a Bridging Model," *Direct and Large-Eddy Simulation-III*, P. R. Voke, N. D. Sandham, and L. Kleiser (eds.), Kluwer, pp. 225-236.

Germano, M., 2001, "LES Overview," in *DNS/LES Progress and Challenges*, C. Liu, L. Sakell, and T. Beutner (eds.), Greyden Press, Columbus, OH, pp. 1-12.

Germano, M., Piomelli, U., Moin, P., and W. H. Cabot 1991, "A Dynamic Subgrid-Scale Eddy Viscosity Model," *Phys. Fluids A*, Vol. 3, pp. 1760-1765.

Moin, P., and Jimenez, J., 1993, "Large-Eddy Simulation of Complex Turbulent Flows," *AIAA Paper No. 93-3099.*

Pruett, C. D., 2000, "On Eulerian Time-Domain Filtering for Spatial Large-Eddy Simulation," *AIAA J.*, Vol. 38, pp. 1634-1642.

Pruett, C. D., 2001, "Toward the De-Mystification of LES," *DNS/LES Progress and Challenges*, C. Liu, L. Sakell, and T. Beutner (eds.), Greyden Press, Columbus, OH, pp. 231-238.

Pruett, C. D., Adams, N. A., and Sochacki, J. S., 2001, "On Taylor-Series Expansions of Residual Stress," *Phys. Fluids*, Vol. 13, pp. 2578-2589.

Stolz, S., and Adams, N. A., 1999, "An Approximate Deconvolution Procedure for Large-Eddy Simulation," *Phys. Fluids A*, Vol. 11, pp. 1699-1701.

Vasilyev, O. V., Lund, T. S., and Moin, P., 1998, "A General Class of Commutative Filters for LES in Complex Geometries," *J. Comput. Phys.*, Vol. 141, pp. 82-104.

Vreman, B., Geurts, B., and Huerten, H., 1994, "Realizability Conditions for the Turbulent Stress Tensor in Large-Eddy Simulation," *J. Fluid Mech.*, Vol. 278, pp. 351-362.